Desalination and Water Treatment
www.deswater.com

doi: 10.5004/dwt.2019.23776

146 (2019) 1–7
April

Effects of the selectivity coefficient on the kinetics of Donnan separation

Hilla Shemer*, Abraham Sagiv, Raphael Semiat, David Hasson

GWRI Rabin Desalination Laboratory, Department of Chemical Engineering, Technion-Israel Institute of Technology, Haifa 3200003, Israel, Tel. +972 4 8292488; emails: shilla@technion.ac.il (H. Shemer), sagiv.ar@gmail.com (A. Sagiv), cesemiat@technion.ac.il (R. Semiat), hasson@technion.ac.il (D. Hasson)

Received 24 December 2018; Accepted 11 Janaury 2019

ABSTRACT

The objective of this study was to enable precise evaluation of Donnan separations, under diffusion controlled conditions, using the ion exchange membrane selectivity coefficient, *Kc*. This was accomplished by experimental measurement of the selectivity of Selemion® AMV anion–exchange membrane toward nitrate, bicarbonate, phosphate and sulfate, and analyzing batch Donnan separations data of these target ions with NaCl stripping solution according to flux equations which take into account the membrane selectivity. By fitting the experimental separation data to the model equations, kinetic coefficients characterizing the Donnan dialysis were determined for both the simplified case of *Kc* = 1 and for the more precise case based on the experimental *Kc* value. The difference in the kinetic coefficient based on the simplified case of *Kc* = 1 and on the experimental *Kc* value is around 10% for sulfate ions, 20% for the nitrate and bicarbonate ions and approximately 40% for the phosphate. These differences may cause deviation in evaluating the time required to achieve a desired target ion removal.

Keywords: Donnan dialysis; Flux modeling; Ion exchange membrane; Membrane selectivity; Diffusion

1. Introduction

Donnan dialysis process utilizes diffusion of target–ions through an ion exchange membrane (IEM) to attain separation or concentration of ionic species. Ion exchange membranes bear fixed charges in the polymer matrix which allow passage of the oppositely charged target–ions from a feed solution to a receiver solution with counter migration of stripping counter–ions from the receiver to the feed [1–6]. Transfer of target – ions from the feed solution to the receiver solution involves the following steps: mass transfer of the ions from the solution bulk to the solution membrane interface; migration of the ions from the solution interface into the membrane; diffusion of the ions through the IEM from to its feed side to its receiver side; migration of the ions from the membrane receiver side to the solution interface; mass transfer of the ions from membrane–solution interface to the to the receiver solution [3].

When IEM containing A^{p-} counter ions is introduced to a solution having B^{q-} target ions, the following equilibrium between the membrane and the bulk solution phases is established [6]:

$$qR_pA^- + pB^q \underset{k_2}{\overset{k_1}{\rightleftarrows}} pR_qB^{q-} + qA^- \tag{1}$$

An important IEM property is its affinity to different ions, defined by the selectivity coefficient:

$$K_A^B = \left(\frac{[A]_w}{[A]_m}\right)^q \left(\frac{[B]_m}{[B]_w}\right)^p = \frac{k_1}{k_2} \tag{2}$$

where K_A^B is the selectivity coefficient with regards to ions B and A; the indices w and m refers to the concentration at the solution side of the membrane–solution interface the concentration at membrane side respectively.

---

* Corresponding author.

The selectivity coefficient is a measurement of the preference of the IEM membrane toward some ions. The greater the selectivity coefficient, the greater the preference for the ion; B ion is preferred by the membrane for $K_A^B > 1$, while *A* ion is preferred at $K_A^B < 1$. It is reported that the ion–exchange selectivity coefficient is practically independent of ionic composition, so that possible gradients of ionic activity coefficients balance one another and thus have little effect on the ionic fluxes [7].

The mobility of ions in the IEM is controlled by their size, their interaction with the fixed ionic groups and the cross–linking density of the IEM. In general, ions with higher valence and smaller hydrate radius have a higher permeability compared with ions with lower valance and larger hydrate radius [2,8]. The preference of the higher valence ion is explained by the Donnan potential which is proportional to the ion valence [9]. Ions with different hydrated radii may be differentiated based on a size sieving effect. The generalization that ions with smaller hydrate radius are preferred by the IEM is not always valid. For larger ions the sieving effect in some IEM membranes cancels the electro–selectivity and therefore, the permeability these ions is significantly reduced [8]. Non–ionic van der Waals or hydrophobic interactions between the ions and the matrix can also affect binding [9].

The selectivity coefficient may influence the flux of a target–ion through an IEM due to its effect on the intra–membrane interfacial concentrations. Velizarov et al. [10] conducted a theoretical analysis of the effect of the selectivity coefficient on the flux of nitrate through Neosepta ACS membrane. They showed that the flux increased with the selectivity of the membrane toward nitrate with chloride as a counter ion from $K_{Cl}^{NO_3} = 1$ to 5, after which the increase in the flux was modest up to $K_{Cl}^{NO_3} = 10$. This was explained by the decreasing weight of the membrane–associated resistance in the flux equation.

The simple Donnan dialysis model derived in our previous publications [4,5] was based on the simplifying assumption that the membrane selectivity coefficient *Kc* is equal to 1. The objective of this study was to enable more precise evaluation of Donnan separations using measured *Kc* values. This was accomplished by experimental measurement of the selectivity of Selemion® AMV anion–exchange membrane toward nitrate, bicarbonate, phosphate, and sulfate and analyzing batch Donnan separations data of theses target ions with NaCl stripping solution according to modified equations which take into account the membrane selectivity. When the mass transfer coefficients and/or the solution concentrations are relatively low the kinetics of the Donnan system is controlled by mass transport of the ions through the boundary layers at the two membrane sides. Under these conditions, the magnitude of the selectivity coefficient has a negligible effect on the Donnan separation. The magnitude of the selectivity coefficient has an effect on the Donnan separation only in the case of diffusional transport control.

2. Flux rate equation under diffusion controlled conditions

The following mass balances constrain a system of a KB salt in the feed solution and NaA salt in the receiver solution. In the analysis presented herein, the target–ion B^{q-} may be monovalent (*q* = 1) or divalent (*q* = 2) while the counter ion A^- is monovalent. The concentration change with time, in a batch mode operation of a dialyzer for monovalent ions, is given by the following dimensional differential equation in which *Kc* = 1 [4]:

$$-\frac{d[\mathrm{B}^-]_1}{dt} = \frac{S}{V_F}\cdot P_s\left\{\frac{[\mathrm{B}^-]_1}{[\mathrm{K}^+]_0} - \frac{[\mathrm{B}^-]_2}{[\mathrm{Na}^+]_0}\right\} \tag{3}$$

where *S* is the membrane area (cm²), V_F is the feed solution volume (mL), P_s is the overall kinetic coefficient (mol/m² h; $P_S = [X_m{}^+]\cdot D_m / \delta$), $[X_m{}^+]$ is the exchange capacity (mol/m³), D_m is the membrane diffusion coefficient (m²/h), δ_m is the membrane thickness (m), $[B^-]_1$, and $[B^-]_2$ are the target–ion concentrations in the feed and receiver respectively (mmol/L), $[Na^+]_0$ and $[K^+]_0$ are the initial NaA and KB salts concentration in the feed and receiver respectively (mmol/L).

The concentration change for the divalent target–ion is given by [5]:

$$-\frac{d[\mathrm{B}^{2-}]_1}{dt} = \frac{S}{V_F}\cdot P_m\left\{[\mathrm{B}^{2-}]_{m_1} - [\mathrm{B}^{2-}]_{m_2}\right\} \tag{4}$$

where $[B^{2-}]_{m_1}$, and $[B^{2-}]_{m_2}$ are the target–ion concentrations on the membrane feed and receiver sides respectively, (mmol/L) and P_m is the membrane permeability coefficient (m/h; $P_m = D_m/\delta_m$).

The following electro–neutrality and mass balance conditions were used in solving the earlier equations, as explained in detail elsewhere [4,5]:

$$[\mathrm{K}^+]_0 = q[\mathrm{B}^{q-}]_0 = q\left([\mathrm{B}^{q-}]_1 + [\mathrm{B}^{q-}]_2\right) = q[\mathrm{B}^{q-}]_1 + [\mathrm{A}^-]_1 \tag{5}$$

$$[\mathrm{Na}^+]_0 = [\mathrm{A}^-]_0 = [\mathrm{A}^-]_1 + [\mathrm{A}^-]_2 = [\mathrm{A}^-]_2 + q[\mathrm{B}^{q-}]_2 \tag{6}$$

$$q[\mathrm{B}^{q-}]_{m_1} + [\mathrm{A}^-]_{m_1} = [\mathrm{X}_m^+] \tag{7}$$

$$q[\mathrm{B}^{q-}]_{m_2} + [\mathrm{A}^-]_{m_2} = [\mathrm{X}_m^+] \tag{8}$$

The selectivity coefficients in both the feed and receiver sides are given by:

$$Kc_{\mathrm{A}^{q-}}^{\mathrm{B}-} = \left(\frac{[\mathrm{A}^-]_1}{[\mathrm{A}^-]_{m_1}}\right)^q \frac{[\mathrm{B}^{q-}]_{m_1}}{[\mathrm{B}^{q-}]_1} \tag{9}$$

$$Kc_{\mathrm{A}^{q-}}^{\mathrm{B}-} = \left(\frac{[\mathrm{A}^-]_2}{[\mathrm{A}^-]_{m_2}}\right)^q \frac{[\mathrm{B}^{q-}]_{m_2}}{[\mathrm{B}^{q-}]_2} \tag{10}$$

where subscripts 1 and 2 represent feed and receiver solutions respectively, subscript *m* is the concentration on the membrane side.

The final equations for the monovalent and divalent target ions, which include the selectivity coefficient *Kc*, are as follows:

$$-\frac{d[\mathrm{B}^-]_1}{dt} = P_S \cdot \frac{S}{V_F}\left\{ \frac{[\mathrm{B}^-]_1 - \left\{ \dfrac{[\mathrm{K}^+]_0^2}{[\mathrm{K}^+]_0 + [\mathrm{Na}^+]_0} \right\}}{\begin{array}{c} \left\{ \left(\dfrac{[\mathrm{K}^+]_0}{[\mathrm{K}^+]_0 + [\mathrm{Na}^+]_0} \right) + \left([\mathrm{B}^-]_1 \dfrac{(Kc-1)}{[\mathrm{K}^+]_0 + [\mathrm{Na}^+]_0} \right) \right\} \\ \left\{ \dfrac{[\mathrm{Na}^+]_0 + (Kc-1)\left([\mathrm{K}^+]_0 - [\mathrm{B}^-]_1\right)}{Kc} \right\} \end{array}} \right\} \tag{11}$$

$$-\frac{d[\mathrm{B}^{2-}]_1}{dt} = \frac{S}{V_F} \cdot P_m \cdot \left\{ \begin{array}{l} \left(\dfrac{-1 + \sqrt{1 + \dfrac{8Kc[\mathrm{K}_m^+][\mathrm{B}^{2-}]_1}{\left([\mathrm{Na}^+]_0 - \dfrac{[\mathrm{B}^{2-}]_1}{2} \right)^2}}}{\dfrac{8Kc[\mathrm{B}^{2-}]_1}{\left([\mathrm{Na}^+]_0 - \dfrac{[\mathrm{B}^{2-}]_1}{2} \right)^2}} \right) - \\ \left(\dfrac{-1 + \sqrt{1 + \dfrac{8Kc[\mathrm{K}_m^+]\left(\dfrac{[\mathrm{Na}]_0}{2} - [\mathrm{B}^{2-}]_1 \right)}{\left([\mathrm{K}^+]_0 - [\mathrm{Na}^+]_0 + 2[\mathrm{B}^{2-}]_1 \right)^2}}}{\dfrac{8Kc\left(\dfrac{[\mathrm{Na}^+]_0}{2} - [\mathrm{B}^{2-}]_1 \right)}{\left([\mathrm{K}^+]_0 - [\mathrm{Na}^+]_0 + 2[\mathrm{B}^{2-}]_1 \right)^2}} \right) \end{array} \right\} \tag{12}$$

3. Experimental setup

3.1. Ion exchange membrane properties

Selemion® AMV anion exchange membrane, obtained from Asahi Glass (Japan), was used. The membrane properties are as follows: thickness $\delta = 0.012$ cm; ion exchange capacity = 1.85 meq/g; density $\rho = 1.09$ g/cm³; and exchange capacity $[X_m^+] = 2016$ mol/m³.

3.2. Kc determination

The selectivity coefficients of nitrate, phosphate, bicarbonate, and sulfate, were determined according to the method of Vyas et al. [11]. In brief, cut–off samples of the membrane (4 × 4 cm²) were conditioned for 48 h using 1 M HCl followed by 48 h with 0.1 M NaCl solution. A membrane sample was then immersed in a solution containing a certain target ion concentration mixed with 15 mmol/L of NaCl solution in a water bath (100 rpm), at 25°C, until equilibrium was achieved. The residual target ion concentration enabled determination of *Kc* (Eq. (2)).

The target–ion concentrations examined in the *Kc* and Donnan separations are listed in Table 1. A total of 10–15 replicates (with different membrane pieces) were carried out for each target–ion *Kc* determination. In the phosphate and bicarbonate experiments, the presence of monovalent ions was ensured by controlling the solution pH values at 5.8 and 7.8 respectively, which provided over 96% of the monovalent species.

3.3. Donnan dialysis kinetics

Dialysis experiments were performed to measure the target–ions change with time under diffusion–controlled conditions. A batch recycle system, described in detail elsewhere [4,5], was used. The receiver solution was filled in all runs with 2 L of 1,000 mmol/L NaCl. The feed solution was filled with 2 L of a target ion concentration in the range listed in Table 1.

3.4. Analytical methods

The analyses of phosphate and sulfate ions were carried out using Hach DR2800 spectrophotometer methods 8048 and 8051 respectively. Nitrate ions concentration was determined by direct absorption measurements at λ = 220 nm (Evolution 201 UV-VIS spectrophotometer, Thermo Scientific). Bicarbonate was determined using HCl titration (Method 2320B [12]).

4. Results

4.1. Kc values

Fig. 1 displays experimental *Kc* values obtained for various inlet concentrations of nitrate, phosphate, bicarbonate, and sulfate solutions, with chloride as a counter–ion. It is seen that the initial target–ions concentration did not affect the *Kc* values. Similar results were reported by Vyas at al. [11]

Table 1
Experimental conditions for *Kc* and Donnan dialysis

Anion	Concentrations (mmol/L)		pH
	Kc exp.	Donnan exp.	
NO_3^-	0.5–4.0	23–82	7.1
HCO_3^-	0.6–4.2	21–77	7.8
$H_2PO_4^-$	0.1–0.2	22–91	5.8
SO_4^{2-}	1.0–4.5	25–40	7.1

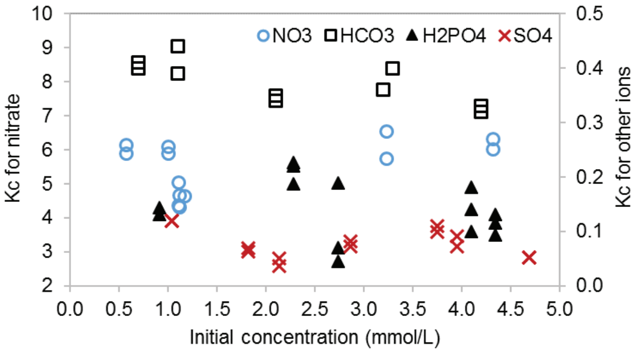

Fig. 1. *Kc* as a function of the initial target ions concentration.

and Malewitz et al. [13]. The average calculated value of the selectivity coefficients are displayed in Table 2. For the nitrate ion *Kc* > 1, indicating its preference by the membrane compared with the other three ions at which the experimental *Kc* < 1. The high *Kc* value of nitrate can be partially attributed to the higher stability of nitrate within the less hydrated environment of the membrane matrix [10].

Overall, the selectivity coefficients follow the order of $NO_3^- \gg HCO_3^- > H_2PO_4^- > SO_4^{2-}$. This anion selectivity order does not follow the trend of the hydrated radii but rather the trends of the thermochemical radii and the diffusion coefficients, all listed in Table 2. It is seen that the higher the diffusion coefficient the higher the *Kc* of the monovalent ions. Additionally, the selectivity sequence reflects the hydrophobicity of the aqueous anion. The larger the thermochemical radius, and the lower the charge density and hydration energy, the more hydrophobic the ion [9]. Among the monovalent ions, phosphate has the larger thermochemical radius, (i.e., lower charge density and hydration energy) while nitrate has the lowest thermochemical radius. It can be therefore, concluded that the preference of the Selemion® AMV membrane toward hydrophobic anions is low.

It is more difficult to compare the selectivity preference between monovalent and divalent ions across charge and hydrophobic characteristics [9]. The results in Table 2 indicate that sulfate had the lowest selectivity coefficient due to its largest thermochemical radius. It is also reported that a resin with large spacing between functional groups, is more selective to monovalent ions than to divalent ions as the wide spacing can be easily accessed by monovalent ions and favorably interact with charged sites [14].

Table 3 lists the *Kc* values extracted from the literature for the studied target–ions with chloride as a counter ion. The experimental values of this study are seen to be within the range of values reported in the literature. The deviating high *Kc* values for phosphate and sulfate reported by Beck and Ernst [15] are based on Donnan separation results measured in the experimental system of this study. While their *Kc* values were derived by fitting the Donnan separation results to a theoretical model the *Kc* data of this study are direct experimental observations. The low *Kc* values of nitrate and bicarbonate, reported by Wiśniewski and Różańska [18], for both Selemion® AMV and Neosepta AMX membranes might suggest that they were measured at high ionic strength solutions, as these values

Table 2
Experimental *Kc* (Kc_{obs}) hydrated radii and diffusion coefficient of the tested ions

Anion	Kc_{obs}	Hydrated radii (nm) [16]	Thermochemical radii (nm) [17]	Diffusion coefficients (10^{-10} m²/s) [16]
NO_3^-	5.51 ± 0.79	0.335	0.200	19.2
HCO_3^-	0.37 ± 0.04	0.210	0.207	11.9
$H_2PO_4^-$	0.14 ± 0.05	0.490	0.213	9.6
SO_4^{2-}	0.08 ± 0.03	0.379	0.218	10.7

Table 3
Literature values of *Kc* for various ion exchange membranes (temperature and ionic concentrations in brackets)

Membrane	K_{Cl}^{B}				Reference
	NO_3^-	HCO_3^-	$H_2PO_4^-$	SO_4^{2-}	
Selemion® AMV	5.51	0.37	0.14	0.08	This research (25°C; 0.02 M)
	5.5 ± 0.20		3.7 ± 0.15	5.3 ± 0.15	[15] (na)
	4.3				[13] (25°C, 0.1 M)
	0.095	0.047		0.186	[18] (na)
Neosepta AMX	4.1				[13] (25°C, 0.1 M)
	0.109	0.018		0.011	[18] (na)
	2.86 (0.1 M)			3.49 (0.1 M)	[19] (25°C)
	1.71 (0.2 M)			2.03 (0.2 M)	
	0.29 (0.3 M)			0.06 (0.3 M)	
	0.15 (0.5 M)			0.02 (0.5 M)	
	0.48 (10°C)			0.03 (10°C)	[20] (0.3 M)
	0.71 (25°C)			0.11 (25°C)	
	1.10 (40°C)			0.29 (40°C)	
Neosepta AFN	5.25	0.31		1.97	[18] (na)
Neosepta ACS	4.1				[21] (na)
	1.85				[19] (25°C; 0.1 M)
Dowex 1x8 resin	5.77			0.07	[22] (25°C; 0.3 M)

correspond to the values measured by Louati et al. [19] at a solution of 0.5 M. Nonetheless, the conditions as which the *Kc* values were determined were not specified by the authors.

The literature data presented in Table 3 indicate that *Kc* values depend on ionic strength of the aqueous solution, the temperature, and membrane type. Louati et al. [19] showed that as the ionic strength increases the selectivity of Neosepta AMX membrane toward the counter–ions (chloride) raised. These results were explained by a decrease of the electrostatic potential of the membrane surface with the increase of the solution ionic strength. As temperature rises the *Kc* value increases due to the endothermic nature of the ion exchange reactions (Eq. (1)). The Van't Hoff equation also shows that the selectivity coefficient increases with temperature [20]. A strong dependence between membrane selectivity and the pore–wall charge density (a characteristics of membrane structure) was reported by Malewitz et al. [13].

4.2. Kinetic coefficients

The simple Donnan dialysis model derived in our previous publications [4,5] was based on the simplifying assumption *Kc* = 1. The availability of experimental *Kc* coefficients enables more precise evaluation of Donnan separations according to the equations, presented herein, which take into account the membrane selectivity. The experimental data, of transfer of the target ion from feed to receiver as a function of time, were analyzed according to the batch integrated Eq. (11) for the monovalent ions to provide values of the kinetic coefficient P_s for both the simplified case of *Kc* = 1 and the more accurate case based on the experimental value of *Kc* (Kc_{obs}). Similarly, the divalent data were analyzed according to the batch integrated Eq. (12) to provide values of the permeability coefficient P_m for both *Kc* = 1 and Kc_{obs} value. For each of the *Kc* values the kinetic or permeability coefficient was evaluated by the minimal deviation between calculated and experimental concentration using the least squares method. Fig. 2 illustrates typical deviations experimental between experimental measurements and calculated separation curves based on *Kc* = 1 and on the measured value of *Kc*.

Fig. 3 and Tables 4 and 5 summarize the values of the kinetic coefficients and of the permeability coefficient as a function of feed concentration. The kinetic coefficients are seen to increase with the concentration of the target–ions. This phenomenon was also observed in other membranes types and related to the increase in membrane ion diffusivity with solution concentration [4].

The difference in the kinetic coefficient *Ps* calculated at *Kc* = 1 and at the experimental *Kc* is around 20% for nitrate and bicarbonate, approximately 40% for phosphate, and about 10% for sulfate. These differences cause deviations in the evaluation of the time required to achieve certain degree of the target–ion transfer (Fig. 2). For example, the estimated times to achieve 80% removal of nitrate, from initial concentration 23 mmol/L, are 8 h for *Kc* = 1 and 9 h for *Kc* = 5.5. In this case, the agreement between experimental and predicted

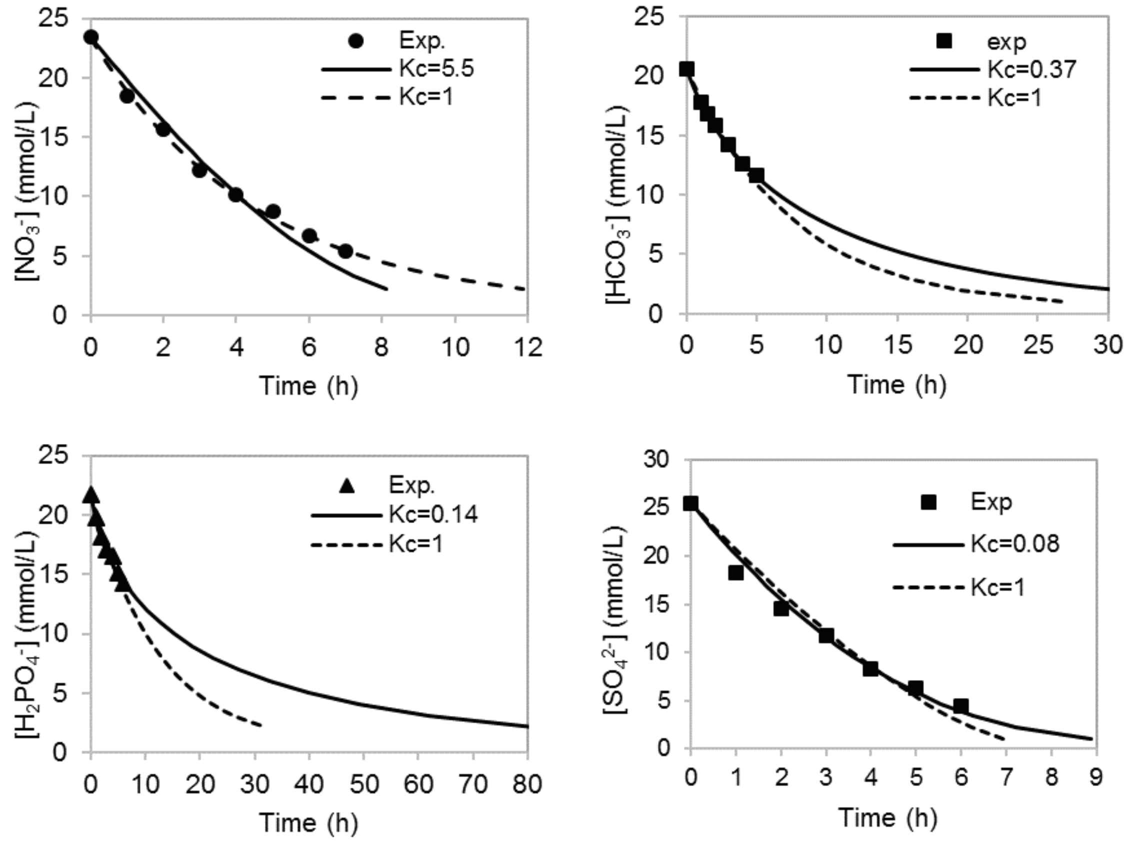

Fig. 2. Predicted concentration change with time for *Kc* = 1 and measured *Kc* (initial target–ions concentration of 20 mmol/L and receiver NaCl concentration of 1,000 mmol/L).

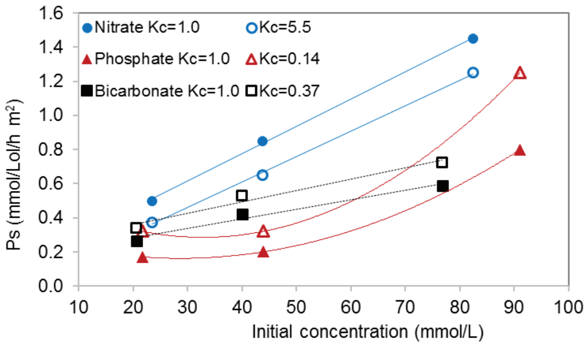

Fig. 3. Kinetic coefficients as a function of the initial target–ions concentrations.

Table 4
Overall kinetic coefficients (*Ps*) of the monovalent target–ions at *Kc* = 1 and experimental *Kc*

Anion	Concentration (mmol/L)	*Ps* (mol/m² h)		Value of Kc_{obs}
		Kc = 1	Kc_{obs}	
NO_3^-	23.4	0.50	0.38	5.5
	43.8	0.85	0.65	
	82.5	1.45	1.25	
HCO_3^-	20.6	0.27	0.34	0.37
	40.0	0.42	0.53	
	76.8	0.59	0.73	
$H_2PO_4^-$	21.8	0.17	0.32	0.14
	43.9	0.20	0.32	
	91.1	0.80	1.25	

Table 5
Permeability coefficients (*Pm*) of sulfate at *Kc* = 1 and experimental *Kc*

Anion	Concentration (mmol/L)	Pm (10^{-4} m/h)	
		Kc = 1	Kc_{obs} = 0.08
SO_4^{2-}	25.5	1.50	1.70
	38.5^a	2.78 ± 0.22	2.98 ± 0.27

^{a}Average value of four experiments.

values seems better for *Kc* = 1. The difference of the *Pm* values for *Kc* = 1 and the experimental *Kc* of sulfate is 11.8% for initial concentrations of 25 mmol/L. The predicted times for 80% sulfate removal are close at 6.0 and 7.3 h for *Kc* = 1 and *Kc* = 0.08 respectively. A better fit between experimental and predicted values were obtained for the measured *Kc* of 0.08.

It is expected that the extent of the time differences would increase in the case of 90% removal of bicarbonate and phosphate. In the experiments, only about 40% transfer of both ions was achieved. Theoretically, at *Kc* = 1 a predicted duration of 32.1 h is obtained to achieve 90% removal of 22 mM phosphate, as compared with 81.7 h at *Kc* = 0.14. For bicarbonate at the initial concentration of 21 mM, the durations are 31.1 h for *Kc* = 1 and 19.5 h for *Kc* = 0.37.

5. Conclusions

The main contribution of this research is to enable improved evaluation of Donnan separations by taking into account the membrane selectivity coefficients. A selectivity coefficient *Kc* > 1 was measured for nitrate while *Kc* < 1 was measured for bicarbonate, phosphate, and sulfate. Transport of these target–ions through the anion exchange membrane was modeled to include the selectivity coefficients, under diffusion–controlled conditions, at which the selectivity coefficient affects the transport. The modified transport model showed a more accurate model based on experimental selectivity coefficients.

Acknowledgments

The research was supported by the Israel Science Foundation Grant No. 1766/17.

References

[1] T.A. Davis, Donnan dialysis. Encyclopedia of Desalination and Water Resources Vol. 2 Membranes, Eolss Publishers Co., U.K., 2010, pp. 230–241.
[2] T. Luoa, S. Abdua, M. Wessling, Selectivity of ion exchange membranes: a review, J. Membr. Sci., 555 (2018) 429–454.
[3] S. Sarkar, A.K. Sengupta, P. Prakash, The Donnan membrane principle: opportunities for sustainable engineered processes and materials, Environ. Sci. Technol., 44 (2010) 1161–1166.
[4] D. Hasson, A. Beck, F. Fingerman, C. Tachman,, H. Shemer, R. Semiat, Simple model for characterizing a Donnan dialysis process, Ind. Eng. Chem. Res., 53 (2014) 6094–6102.
[5] S. Ring, D. Hasson, H. Shemer, H. Semiat,Simple modeling of Donnan separation processes, J. Membr. Sci., 476 (2015) 348–355.
[6] F. Helfferich, Ion Exchange. McGraw-Hill, NY, 1962, p. 153.
[7] F. Helfferich, Ion-exchange kinetics. III. Experimental test of the theory of particle-diffusion controlled ion exchange, J. Phys. Chem., 66 (1962) 39–44.
[8] H. Strathmann, Ion-Exchange Membrane Separation Processes, Elsevier, 2004 p.79.
[9] Y. Hu,, J. Foster, T.H. Boyer, Selectivity of bicarbonate-form anion exchange for drinking water contaminants: influence of resin properties, Sep. Purif. Technol., 163 (2016) 128–139.
[10] S. Velizarov, M.A. Reis, J.G. Crespo, Removal of trace monovalent inorganic pollutants in an ion exchange membrane bioreactor: analysis of transport rate in a denitrification process, J. Membr. Sci., 217 (2003) 269–284.
[11] P.V. Vyas, P. Ray, G.S. Trivedi, S.K. Adhikary, R. Rangarajan, Studies on exchange equilibria of cations between cation-exchange membranes and electrolytic solutions, J. Colloid Interf. Sci., 246 (2002) 366–371.
[12] APHA, Standard Methods for Water and Wastewater Examination, 21st Ed, American Public Health Association, Washington DC, USA, 2005.
[13] T. Malewitz, P.N. Pintauro, D. Rear,Multicomponent absorption of anions in commol/Lercial anion-exchange membranes, J. Membr. Sci., 301 (2007) 171–179.
[14] D. Clifford, W.J. Weber, The determinants of divalent/monovalent selectivity in anion exchangers, React. Polym., 1 (1983) 77–89.
[15] A. Beck, M. Ernst, Kinetic modeling and selectivity of anion exchange in Donnan dialysis, J. Membr. Sci., 479 (2015) 132–140.
[16] P. Mondal, A.T.K. Tran, B. Van der Bruggen, Removal of As(V) from simulated groundwater using forward osmosis: effect of competing and coexisting solutes, Desalination, 348 (2014) 33–38.
[17] M.C. Simoes, K.J. Hughes, D.B. Ingham, L. Ma, M. Pourkashanian, Estimation of the thermochemical radii and ionic volumes of complex ions, Inorg. Chem., 56 (2017) 7566–7573.
[18] J. Wiśniewski, A. Różańska, Donnan dialysis with anion-exchange membranes as a pretreatment step before electrodialytic desalination, Desalination, 191 (2006) 210–2018.

[19] I. Louati, F. Guesmi, C. Hannachi, B. Hamrouni, Modification of the AMX membrane surface by polyethyleneimine: effect of ionic strength on the membrane ion exchange selectivity, Can. J. Chem. Eng., 94 (2016) 2386–2393.
[20] F. Guesmi, C. Hannachi, C. Hamrouni, Effect of temperature on ion exchange equilibrium between AMX membrane and binary systems of Cl^-, NO_3^- and SO_4^{2-} ions, Desalin. Wat. Treat., 23 (2010) 32–38.
[21] D. Nwal Amang, S. Alexandrova, P. Schaetzel, Bi-ionic chloride-nitrate equilibrium in a commol/Lercial ion-exchange membrane, Desalination, 159 (2003) 267–271.
[22] C. Hannachi, F. Guesmi, K. Missaoui, H. Tounakti, B. Hamrouni, Ion Exchange Equilibrium between DOWEX 1X8 Resin Modified by Polyethyleneimine and Electrolyte Solutions, J. Water Res. Protect., 5 (2013) 1059–1065.